Amino Acids (2013) 45:1073–1087
DOI 10.1007/s00726-013-1585-y

MINIREVIEW ARTICLE

Current advances in research of cytochrome *c* oxidase

Dragan M. Popović

Received: 13 May 2013 / Accepted: 21 August 2013 / Published online: 3 September 2013

Abstract The function of cytochrome *c* oxidase as a biomolecular nanomachine that transforms energy of redox reaction into protonmotive force across a biological membrane has been subject of intense research, debate, and controversy. The structure of the enzyme has been solved for several organisms; however details of its molecular mechanism of proton pumping still remain elusive. Particularly, the identity of the proton pumping site, the key element of the mechanism, is still open to dispute. The pumping mechanism has been for a long time one of the key unsolved issues of bioenergetics and biochemistry, but with the accelerating progress in this field many important details and principles have emerged. Current advances in cytochrome oxidase research are reviewed here, along with a brief discussion of the most complete proton pumping mechanism proposed to date, and a molecular basis for control of its efficiency.

Keywords Cytochrome *c* oxidase · Proton pumping mechanism · Kinetic control · Proton-coupled electron transfer · Catalytic cycle · Bioenergetics · Redox-driven proton pump

Abbreviations

CcO	Cytochrome *c* oxidase
ET	Electron transfer
PT	Proton transfer
BNC	Binuclear center
PLS	Proton-loading site
PRAa_3	Propionate A of heme a_3
PRDa_3	Propionate D of heme a_3
DFT	Density functional theory
MD	Molecular dynamic
Pmf	Protonmotive force

Structure and function

Cytochrome *c* oxidase (CcO), as the terminal enzyme of the respiratory electron transport chain, is located in the inner mitochondrial membrane of eukaryotes or plasma membrane of many prokaryotes. Since, most of the biological oxygen consumption is catalyzed by the heme-copper oxidases, their importance for the cellular respiration and energy supply in aerobic organisms is essential. CcO catalyses the reduction of dioxygen to water and utilizes the free energy of the redox reaction for proton pumping across the membrane (Antonini et al. 1970; Wikström 1977), generating the electrochemical proton gradient that subsequently drives the synthesis of ATP (Babcock and Wikström 1992; Ferguson-Miller and Babcock 1996; Hosler et al. 2006).

CcO contains four redox-active metal centers: Cu_A, heme *a* (Fe_a), and the binuclear complex consisting of heme a_3 (Fe_{a3}) and Cu_B, see Fig. 1. Electrons supplied to Cu_A by reduced cytochrome *c* are sequentially transferred

Amino acid numbering refers to bovine cytochrome *c* oxidase.

Electronic supplementary material The online version of this article (doi:10.1007/s00726-013-1585-y) contains supplementary material, which is available to authorized users.

D. M. Popović (✉)
Department of Chemistry, Institute for Chemistry, Technology and Metallurgy, University of Belgrade, Njegoševa 12, 11000 Belgrade, Serbia
e-mail: dpopovic@chem.bg.ac.rs; dpopovic@ucdavis.edu

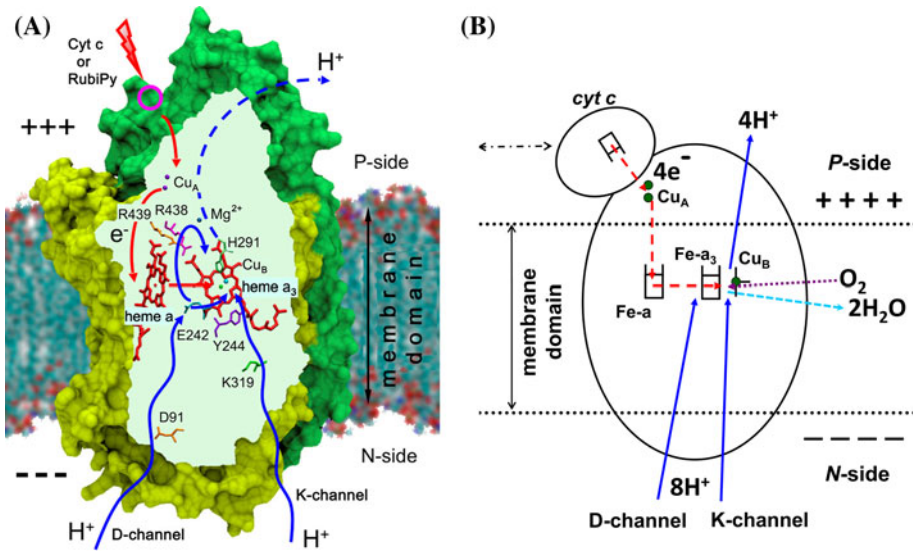

Fig. 1 Structure and function of cytochrome *c* oxidase. **a** Structure of the core subunits of bovine cytochrome oxidase embedded in the mitochondrial membrane. The subunits I and II are displayed by space-filled rendering in *yellow* and *green*, respectively. Metal centers and the key amino acid residues are displayed along with the ET and PT paths shown as *red* and *blue arrows*. Cytochrome *c* and ruthenium(II)-tris-bipyridyl complex are a native and an artificial-photoactive single-electron donors, respectively. **b** The overall reaction catalyzed by CcO. Reduction of O_2 to H_2O is coupled to proton pumping across the membrane against the electrochemical proton gradient

through Fe_a to the active site, where the reduction of oxygen takes place (Ferguson-Miller and Babcock 1996; Konstantinov et al. 1997; Ostermeier et al. 1997). During each turnover (O_2 reduced to water), eight protons are taken up from the inner side of the membrane, four protons being used for water formation in the catalytic site ("chemical or substrate protons") and four protons being pumped across the membrane ("vectorial or pumped protons"). The overall reaction can be expressed as follows:

$$O_2 + 4e^- + 8H^+(in) \longrightarrow 2H_2O + 4H^+(out)$$

where (in) and (out) indicate two sides of the membrane: the inner, negatively charged (*N*-) and the outer, positively charged (*P*-) side, respectively.

The available X-ray structures of cytochrome *c* oxidases indicate three possible pathways for proton conduction within the enzyme: the D-, K- and H-channels (Dürr et al. 2008; Ostermeier et al. 1997; Qin et al. 2009; Svensson-Ek et al. 2002; Tsukihara et al. 2003; Yoshikawa et al. 1998). The putative H-channel is most clearly defined in the structure of the bovine oxidase (Tsukihara et al. 2003) and suggested to have the primary role in translocation of the pumped protons from the *N*- to *P*-side of the membrane (Shimokata et al. 2007). However, mutants designed to examine the role of the H-channel in bacterial oxidases have failed to provide convincing evidence, so far, concerning the functional importance of this putative channel (Lee et al. 2000; Salje et al. 2005). Moreover, many computational studies were not able to find any significant correlation between residues in the H-channel and proton pumping (Fadda et al. 2008; Kaila et al. 2008; Popovic and Stuchebrukhov 2004a; Wikström et al. 2003). In contrast, studies utilizing site-directed mutants provide strong evidence that the D-channel and K-channel are functionally important (Konstantinov et al. 1997; Wikström et al. 2000; Zaslavsky and Gennis 2000). Mutants in the K-channel are clearly defective in one or more steps associated with the reductive halve of the catalytic cycle, i.e., the reduction of the Fe_{a3}/Cu_B binuclear center (Ädelroth et al. 1998; Brändén et al. 2001, 2002; Hosler et al. 1996). Mutants in the D-channel are defective in steps following the interaction of dioxygen with the reduced Fe_{a3}/Cu_B center i.e. during the oxidative halve (Ädelroth et al. 1997; Fetter et al. 1996; Mills et al. 2000; Svensson-Ek et al. 2002). Based on the results of mutagenic studies, 6–7 protons are presumably delivered along the D-channel, whereas the D-channel provides all pumped protons. The rest, one or two chemical protons are provided by the K-channel in the reductive phase of the catalytic cycle (Kirchberg et al. 2013; Ruitenberg et al. 2000, 2002).

During last 40 years, based on many experimental measurements, calculations, computer simulations, and theoretical studies, it has been suggested a variety of different models to explain the pumping mechanism of this complex protein system, see e.g. (Bloch et al. 2004; Brzezinski and Ädelroth 2006; Das et al. 1999; Fadda et al. 2008; Faxen et al. 2005; Kaila et al. 2008; Michel 1998; Olsson and Warshel 2006; Popovic and Stuchebrukhov 2004b; Riistama et al.

1997; Sharpe and Ferguson-Miller 2008; Siegbahn and Blomberg 2007; Siletsky et al. 2004; Tsukihara et al. 2003; Wikström 2000, 2003). Although a molecular mechanism of proton pumping of CcO still remains a subject of intense debate, many common features and principles appear in majority of recently proposed models, and they will be reviewed in the present paper. Some recent reviews of the enzyme structure, function and kinetics, can be found in references (e.g. Belevich et al. 2006, 2007; Brzezinski 2004; Brzezinski and Gennis 2008; Dürr et al. 2008; Gennis 2004; Han et al. 2000; Hosler et al. 2006; Qin et al. 2009; Sarti et al. 2012; Siletsky and Konstantinov 2012). Finally, the pumping model, currently accepted by most researchers in the field of oxidase, will be briefly presented.

The heme–copper superfamily

The mitochondrial CcO is a member of the heme–copper superfamily. These enzymes include respiratory oxidases (O_2 reductases) and NO reductases (Pereira et al. 2001, 2008). The major difference among the heme–copper oxidases is in the variation of the heme-types that occupy the low-spin and high-spin sites, which could be heme *a*, heme *b* and heme *o* (Ferguson-Miller and Babcock 1996). Accordingly, among the solved structures it could be distinguished the aa_3-type from bovine (Shinzawa-Itoh et al. 2007; Tsukihara et al. 1996; Yoshikawa et al. 1998), from *Paracoccus denitrificans* (Iwata et al. 1995; Ostermeier et al. 1997), from *Rhodobacter sphaeroides* (Qin et al. 2006; Svensson-Ek et al. 2002), the ba_3-type oxidase from *Thermus thermophilus* (Luna et al. 2008; Soulimane et al. 2000), and the bo_3-type oxidase from *E. coli* (Abramson et al. 2000). All heme–copper oxidases generally share a similar tertiary structure with high sequence similarity of subunit I and the same arrangement of the metal centers—hemes and copper complex within subunit I (Noor and Soulimane 2013).

Although many experimental results, including those from the electrometric studies (discussed in the next section), are obtained for bacterial CcO (from *P. denitrificans* and *R. sphaeroides*), as it has been demonstrated recently, all species of the A-family (aa_3-type) show remarkable structural similarity. Moreover, their microscopic electrostatic and thermodynamic properties of the key amino acid residues are almost identical, which strongly suggest similar mechanism in all these species (Popovic et al. 2010).

Kinetic experiments

The time-resolved optical and electrometric measurements of the membrane potential generated by the enzyme have been very successful techniques to study CcO, obtaining many important information on kinetics of the processes and the sequence of steps in the reaction mechanism (Belevich et al. 2007; Bloch et al. 2004; Jasaitis et al. 1999; Konstantinov et al. 1997; Ruitenberg et al. 2000, 2002; Siletsky et al. 2004; Zaslavsky et al. 1993). Proton transfer through ordered or semi-ordered water molecules is well reflected by the kinetic isotope effect measurements, another useful experimental technique, that is suitable to assign and link the different kinetic phases with the unequal rate constants in mutants and wild type enzyme (Johansson et al. 2011; Karpefors et al. 1999; Salomonsson et al. 2008; Schmidt et al. 2003).

Recently, (Belevich et al. 2007) have measured the kinetics of the membrane potential generated by CcO (from *P. denitrificans*) inserted in vesicules during the O → E transition. Upon a single-electron injection into the enzyme, four kinetic phases are observed: a pure electronic kinetic phase, and three protonic phases, which overlapped with further movement of an electron, parallel to the membrane surface. Phase 1 (10 μs) is associated with electron transfer from Cu_A to Fe_a, thereby moving a fraction of electron to heme *a*. Further electron redistribution between Cu_A, Fe_a, and the Fe_{a3}/Cu_B binuclear center is coupled to three proton transfer reactions, which generate three additional kinetic phases (150 μs, 800 μs i 2,6 ms; Belevich et al. (2007)), see Fig. 2.

Time-resolved electron transfer and vectorial charge translocation in the F → O transition have been studied with the wild type and N98D mutant enzymes (Siletsky et al. 2004). With the wild type oxidase, the F → O transition begins with rapid electron transfer from Cu_A to heme *a* (15 μs), followed by the intermediate (0.4 ms) and slow protonic phases (1.5 ms). In the N98D mutant, only a single protonic phase (0.6 ms) is observed showing the fourfold H/D kinetic isotope effect. Such a large deuterium isotope effect is a feature of the slow phase (1.5 ms) in the wild type (Johansson et al. 2011; Salomonsson et al. 2005, 2008). Presumably, the 0.6 ms electrogenic phase in the N98D mutant corresponds to proton translocation from the inner *N*-side to E242, replacing the *chemical* proton transferred from E242 to the BNC that is here linked to ET from Fe_a to the BNC. The transfer occurs through the D-channel, because it is also observed in the N98D/K319 M double mutant in which the K-channel is blocked (Vygodina et al. 1998). It is concluded that the intermediate electrogenic phase observed in the wild type oxidase is missing in the N98D mutant, in which the enzyme turnover is decoupled from the proton pumping (Dürr et al. 2008; Han et al. 2006; Johansson et al. 2013; Pfitzner et al. 2000; Vakkasoglu et al. 2006). Recent computational studies explored free energy profiles for the H^+ conduction in the D-pathway of the wild type and N98D mutant enzymes

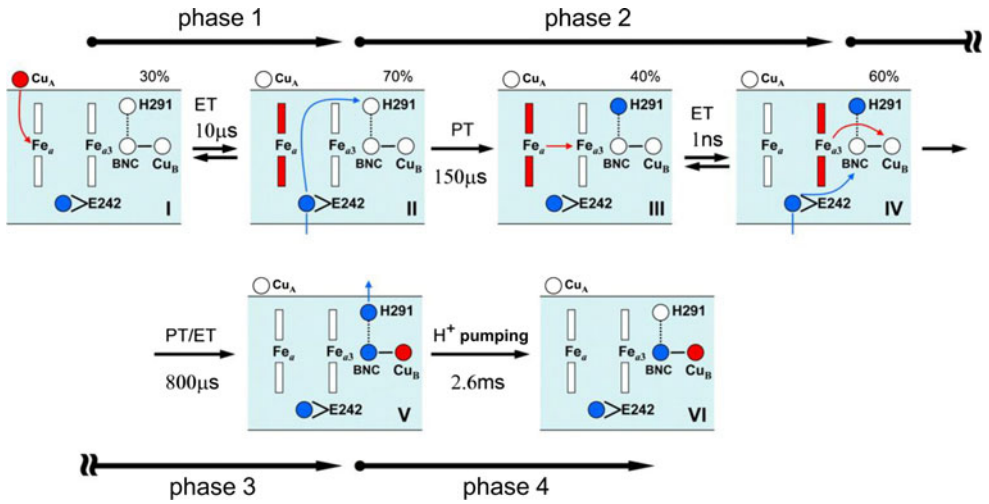

Fig. 2 Schematic interpretation of the kinetic electrometric results for the O → E transition (Belevich et al. 2007). The four redox-active centers (Cu_A, Fe_a, Fe_{a3}, Cu_B) and three key protonatable groups (Glu242, His291, OH^- ligand of the BNC) of the proposed model are schematically shown. The *green fields* represent the membrane domain. The reduced and oxidized metal centers are shown in *red and white color*, while the protonated and deprotonated sites are displayed in *blue and white*, respectively. The *red arrows* represent the electron transfer (ET) steps, as the *blue arrows* represent the proton translocation (PT). Rapid phase 1 is linked to the ET from Cu_A to Fe_a, thereby moving a fraction (70 %) of electron to heme *a*. Phase 2 is a PT from E242 to an unknown PLS above the BNC that is coupled to the ET between heme *a* and the Fe_{a3}/Cu_B center. The ET is incomplete i.e. by the end of 150-μs phase an electron is equilibrated between the two hemes. Phase 3 corresponds to the transfer of the remaining 40 % of an electron from heme *a* to the BNC and an accompanying transfer of the chemical proton to the BNC. Finally, the last 2.6-ms phase is associated with the reprotonation of the donor site for chemical protons and displacement of the pumped proton from the PLS to the *P*-side of the membrane. Presumably, this happens due to repulsion between the chemical proton arrived to the BNC and the pumped proton preloaded to the PLS (Popovic and Stuchebrukhov 2004a; Rich 1995)

emphasizing the importance of protein-bound water molecules for the proton uptake (Henry et al. 2011; Xu and Voth 2006). Significantly, with the wild type oxidase, the protonic phase associated with proton pumping (0.4 ms) precedes the protonic phase associated with the oxygen chemistry (1.5 ms). Moreover, the transfer of the pumped proton to the PLS follows the ET from heme *a* to the BNC, in contrast with the results of the O → E transition.

Key structural elements of the pumping model

One of the key features of the considered model is the existence of the proton-loading site (PLS) located above the heme porphyrins. The identity of PLS has been recently examined in the theoretical kinetic study (Sugitani et al. 2008) showing that only a few sites may play the role—propionates of heme a_3, H291, W126, W236, R438 and R439, all at roughly the same dielectric depth. The identity of the PLS is still not known, but the main candidates are H291 (Popovic and Stuchebrukhov 2004a, b; Sharpe and Ferguson-Miller 2008), PRAa_3 (Kaila et al. 2009; Siegbahn and Blomberg 2007) and PRDa_3 (Fadda et al. 2008; Pisliakov et al. 2008; Wikström 2004; Wikström and Verkhovsky 2007). One model proposed earlier suggests that the pumped proton might be kept distributed between the propionates of heme a_3, H291 and water molecule Wat1 (Fig. 3), including a possible formation of the Zündel-cation ($H_5O_2^+$) or delocalization of a proton on a larger cluster of water molecules in the hydrophilic cavity above the Fea_3/Cu_B complex (Popovic and Stuchebrukhov 2004a).

In addition, the protonation state of the PLS group needs to be linked to the redox state of the binuclear Fe_{a3}/Cu_B complex, although it is not an absolute requirement. The combined DFT/electrostatic calculations (Makhov et al. 2006; Popovic et al. 2005; Quenneville et al. 2004) have shown that H291 is deprotonated if one of metal centers, Fe_{a3} or Cu_B, is oxidized or after the entry of chemical proton and formation of H_2O molecule in the active site. In both cases, there is an additional positive charge present in the BNC, which significantly decreases pK_a of H291 (Ali-Torres et al. 2011; Stuchebrukhov and Popovic 2006). In contrast, H291 is protonated if both metal centers of the BNC are in the reduced form (Popovic et al. 2005; Popovic and Stuchebrukhov 2004a). Similar conclusions are made for PRAa_3 as the PLS in the different models (Blomberg and Siegbahn 2010; Kaila et al. 2009).

CcO is a redox-driven proton pump, where the coupling of electron and proton transfer reactions has a central role. There are, however, different aspects related to the ET and PT reactions in proteins. The ET can be explained by the theory of electron tunneling through the protein matrix (Stuchebrukhov 2003). In contrast, a feasible PT between

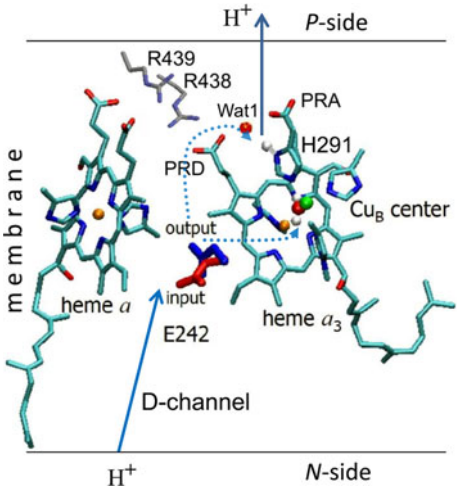

Fig. 3 The key structural elements for the mechanism of proton pumping. Protonation state of the proton-loading site (H291) is linked to the redox state changes in the binuclear Fe_{a3}/Cu_B center. E242 is presumably the main proton donor of chemical and pump protons. Depending on its conformation, E242 can be in protonic contact with the *N*-side through the D-channel, or in contact with oxygen ligands in the BNC, or via a pathway involving the salt bridge ($R438^+/PRDa_3^-$), H_2O (Wat1) and H291 in contact with the *P*-side of the membrane. Water molecules in the D-channel and the catalytic hydrophobic cavity (not shown for clarity) may provide a proton transport pathway and therefore play an important role in the kinetic control of the whole process. By the rotational isomerization (*conformational gating*), E242 controls the *bottom side* of the hydrophobic cavity, whereas the $R438/PRDa_3$ salt bridge controls the *upper side*. In that way it is largely facilitated the unidirectionality of proton and water conduction in CcO

the proton donor and acceptor assumes a presence of the intermediate water molecules and the corresponding hydrogen-bond connectivity, which provides a pathway for the proton translocation by the so-called *Grotthus mechanism* (Agmon 1995).

As established experimentally, the highly conserved E242 plays a central role in conducting both the pumped and chemical protons (Hellwig et al. 1998; Mills et al. 2003; Pawate et al. 2002). In order to transport a proton in the hydrophobic cavity between Glu and PLS or BNC, water molecules are required to provide a pathway and facilitate a proton transfer process. In additon, thermodynamic (Ghosh et al. 2009; Quenneville et al. 2006) and kinetic requirements (Pisliakov et al. 2008; Siegbahn and Blomberg 2007) need to be fulfilled, as well. Though, water molecules are not yet seen in the cavity between the two hemes in the crystal structures of CcO, water is formed in the active site of the enzyme and leaves the catalytic center through that hydrophobic cavity. The free energy calculations suggest that at least four H_2O molecules can be part of the energetically stable structure (Ghosh et al. 2009; Kaila et al. 2008; Pisliakov et al. 2008; Sugitani and Stuchebrukhov 2009; Tashiro and Stuchebrukhov 2005), while the MD studies provide evidence that the two chains of hydrogen-bonded water molecules are formed. One leads from E242 to PRDa_3 and the other branch leads from Glu to the BNC (Zheng et al. 2003). These water molecules are mobile and vibrant, forming the semi-ordered structure, which can get reoriented during the course of the simulation (Wikström et al. 2003). Due to their increased mobility, some of water molecules can interexchange or jump between the two pathways, forming one or other water chain, i.e. to open or close pathways separately (Pisliakov et al. 2008; Sugitani and Stuchebrukhov 2009; Wikström et al. 2005). The two water chains can be in principle utilized to provide the pathways for the PT from E242 to H291 (for the pump protons) and from Glu to OH^- ligand in the BNC (transfer of a chemical proton for reduction of oxygen intermediates).

The proposed "*kinetic gating mechanism*" suggests that E242 is connected to PLS and the active site (BNC) by two separate proton-conducting water chains with different proton-conducting rates. The faster chain delivers the pumped protons to PLS, whereas the slower chain delivers the chemical protons to BNC. The difference in rates ensures that a proton is preloaded into the pump site (PLS) before the driving redox event, i.e. the protonation of the reduced oxygen intermediates at the active site by the chemical protons, occurs (Popovic and Stuchebrukhov 2004b). The structure and dynamics of proton-conducting water networks (Kaila et al. 2008; Olkhova et al. 2004), as well as, electrometric results (Belevich et al. 2007; Bloch et al. 2004; Konstantinov et al. 1997; Siletsky and Konstantinov 2012; Siletsky et al. 2004) suggest that the water network to the PLS has greater proton-conducting rate than the one to the BNC, despite the fact that OH^- ligand in the BNC possesses greater proton affinity than the PLS (H291 or PRAa_3) itself (Kaila et al. 2009; Popovic and Stuchebrukhov 2004a; Quenneville et al. 2006).[1] In other words, the rate of proton transfer from E242 to H291 is much faster than that between E242 and OH^- in the catalytic center. Therefore, it is not here the thermodynamic but rather kinetic criterion that decides a path in which proton is first directed and translocated. As a result, this leads to creation of a meta-stable intermediate state with a preloaded proton at PLS, from which the pumped proton is later ejected (after entry of a chemical proton into the BNC) to the *P*-side of the membrane (Popovic and Stuchebrukhov 2004b, 2005).

From the mechanistic point of view, the salt bridge $R438^+/PRDa_3^-$ and a crystallographically found water

[1] This is particularly pronounce for PRAa_3 as the PLS, since, the aqueous phase pK_as of propionate and OH^- ligand of Cu_B^{2+} complex are 4.8 and 12.5, respectively. Therefore, the reaction and protein field need significantly to shift their pK_a values in order to reverse the order of their proton affinities within the enzyme.

molecule Wat1, located between the propionates of heme a_3 (Fig. 3), are most likely important for the regulation of transfer of the pumped protons to PLS (Lee et al. 2009; Popovic and Stuchebrukhov 2004a). The water molecules are formed as the products of the catalytic reaction and have to leave the active site of the enzyme through the nonpolar cavity. The salt bridge facilitates this process and works as a gate for water exit from the catalytic hydrophobic cavity (Sugitani and Stuchebrukhov 2009; Wikström et al. 2005). Also, the strong salt bridge imposes the thermodynamic obstacles (Popovic and Stuchebrukhov 2005) and kinetic barriers (Blomberg and Siegbahn 2010; Kaila et al. 2009; Siegbahn and Blomberg 2007), which prevent a reverse flow of protons back to the pump (to PLS or to E242).

By rotational isomerization of Glu side-chain, E242 can adopt two distinct conformations—downward and upward, apparently the proton *input* and *output* conformations (Brzezinski and Ädelroth 2006; Popovic and Stuchebrukhov 2006). Due to the thermal fluctuations of the protein and inner water molecules, E242 can flip out from the stable downward conformation to the upward conformation (3–6 kcal/mol less stable; Kaila et al. 2009; Popovic and Stuchebrukhov 2012), facilitating on this way a proton transfer to the PLS or OH^- ligand of the BNC. By flipping back to the downward conformation, on the other hand, Glu can get reprotonated through the D-channel.

If Glu is in its "down" (*input*) conformation, E242 is in protonic contact via protonatable groups in the D-channel with the *N*-side of membrane. When it is in its "up" (*output*) conformation, Glu can transport a proton to the PLS or BNC by establishing the H-bond connectivity via internal water molecules. Thus, in "up" conformation, Glu is in the contact with the *P*-side of membrane, see Fig. 3. Rotational isomerization of the Glu side-chain may be considered as an essential component of the mechanism that prevents simultaneous contact to the pump site, to the site of oxygen reduction and to the proton-conducting D-channel (Fig. 3). Glu can form the H-bonded proton-conducting pathway only to one site at a time, leaving the other two pathways temporarily shutdown. The gating through conformational changes of the Glu side-chain (Popovic and Stuchebrukhov 2006) is similar with the "E242 valve model" proposed by the Wikström group (Kaila et al. 2008).

By MD simulations, Kaila et al. studied the influence of internal water molecules, the redox state of metal centers and electrostatics of the heme propionic groups on the dynamic behavior of E242 in two different protonation states. Glu goes through a protonation state-dependent conformational change, which provides a valve in the pumping mechanism. They emphasized the importance of internal water molecules below and above the E242 side-chain, particularly the fully hydrated state that allows the fast turnover, and discussed the function of the "E242 valve" in terms of controlling and minimizing the back-leakage of protons. This mechanism is mainly concerned with a gating situation, where the pump proton in the PLS has to be prevented from leaking back to Glu^- in the reduced-protonated state of the BNC. The energetics of the two conformations was found to depend on the redox states of the cofactors, as well as the protonation state of E242.

Recent computational study (Yang and Cui 2011) has cast some doubts on the E242 "valve model" and the water-wire gating via water reorientation. This major problem has been also discussed by e.g. Warshel and coworkers (Chakrabarty et al. 2011; Chakrabarty and Warshel 2013; Pisliakov et al. 2008). Electrostatic basis for the unidirectionality of the primary PT from E242 to PRDa_3 was elucidated by calculating the activation barriers of the different steps in several alternative paths, including a leakage from the *P*-side. The EVB and the PDLD/S-LRA semimacroscopic model are used to calculate more accurate energy profiles for proton translocation pathways. Models with different number of water molecules in hydrophobic cavity are examined; moreover, large structural rearrangements and conformational changes of the donor and acceptor group are explored in the MD runs. This work has demonstrated that the proton transfer from E242 to PRDa_3 over several intermediate water molecules in nonpolar hydrophobic region is very expensive and that the reduced number of *bridging* water molecules can actually lower the activation barriers of the PT process.

Kinetic mechanism of proton pumping

Schematic of the proposed proton pumping mechanism is shown in Fig. 4. During the cycle, the stable state of the catalytic center, before an additional electron is supplied to the system, is that in which one of the metal centers is formally oxidized (Fe^{3+}–H_2O or Cu^{2+}–H_2O), while E242 is protonated and H291 (Nδ1 position) is deprotonated.[2] An electron is supplied to the system via cyt *c* to Cu_A and transferred further to heme *a* (step 1), and then to heme a_3–Cu_B binuclear center (step 2). In response to the increased negative charge of the BNC, the proton from E242 has now a driving force to move closer to the catalytic center. There are two proton-conducting pathways leading from E242 to two possible sites: one is leading to OH^- group in the BNC, the second is leading to the deprotonated H291 residue (PLS). Both groups show the high proton affinity, what is revealed by the high values of their pK_as (Popovic

[2] This state is established in a previous step of the cycle, when a chemical proton is accepted by one of the hydroxy ligands of the BNC.

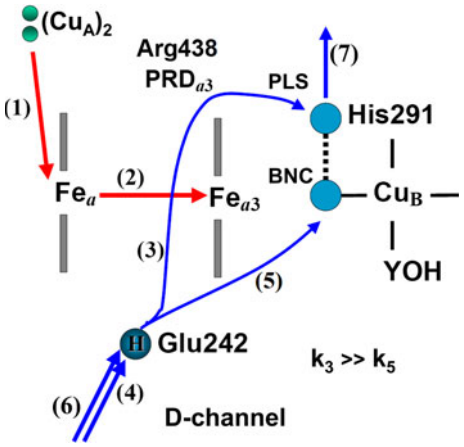

Fig. 4 Schematic of the discussed proton pumping model of CcO. It is shown the sequence of steps during one pumping cycle, i.e. upon the injection of an electron in the system. The PT and ET steps are shown by *blue* and *red arrows*, respectively. In the beginning of the cycle, the proton donor E242 is protonated, while two potential proton acceptors, H291 (PLS) and HO^- ligand of BNC, are deprotonated (*empty circles*). There are two separated proton-conducting water chains—the one leads from Glu to PLS and the other leads to the BNC, which differ in the proton-conducting rates. It is of the essential importance that the proton transfer rate from Glu to PLS along the *pumping path* 3 is much larger than between Glu and OH^- in the BNC along the *chemical path* 5 ($k_3 \gg k_5$), i.e. step 3 occurs before step 5. Otherwise, there is no proton pumping and all protons taken from the *N*-side would be used for the protonation of oxygen intermediates in the BNC

and Stuchebrukhov 2004a; Quenneville et al. 2006). Since the proton translocation rate to H291 is considerably larger than the one to the OH^- group (Belevich et al. 2007; Siletsky and Konstantinov 2012; Siletsky et al. 2004), in the next step the protonation of His occurs, i.e., the transfer of a pump proton to the PLS. Thus, there is here a kinetic (not thermodynamic) control of this PT reaction, what results in formation of a meta-stable state of the enzyme (Popovic and Stuchebrukhov 2004b, 2005) in step 3 (see discussion above). Step 4 is the reprotonation of E242 residue through the D-channel by proton uptake from the *N*-side of the membrane. Now the second *chemical* proton, using a separate path, can be transferred to the BNC protonating OH^- to H_2O (step 5). The presence of an additional positive charge in the BNC consequently decreases the H291 pK_a value (Popovic et al. 2005; Quenneville et al. 2006). Obviously, the entrance of a substrate proton into the active site is an essential component of the pumping mechanism in CcO, since the free energy is generated at the catalytic site. In step 6, E242 presumably the main proton donor of the proton translocation process, once again gets reprotonated through the D-channel. This additionally increases the electrostatic repulsion between a proton at H291 and H_2O ligand in the BNC, what finally, in step 7, leads to ejection of a preloaded proton from the PLS to the *P*-side of the membrane (Popovic and Stuchebrukhov 2006).

Therefore, reprotonation of the proton donor site may control a proton release from the PLS to the *P*-side of the membrane, additionally facilitating the proton pumping event (Brzezinski and Gennis 2008; Popovic and Stuchebrukhov 2006). Moreover, the reprotonation of E242 along with a release of the pumped proton controls entry of the next electron into the enzyme, since the reduction of heme *a* is only feasible if E242 is in the stable protonated state (Popovic and Stuchebrukhov 2012). Such control of the flow of electrons assures that electrons are taken up and consumed one at a time in the active site of the enzyme. Further, it means that the scheme of steps in the pumping mechanism, shown in Fig. 4, cyclically repeats with each new electron entering the system. Since four electrons are required for the complete reduction of O_2 to $2H_2O$, the displayed sequence of steps will be repeated four times to complete the catalytic cycle of the enzyme.

The experimental data for the O → E transition (Belevich et al. 2007) can be interpreted to suggest a mechanism in which the translocation of the pumped proton occurs upon reduction of heme *a* (Brändén et al. 2005), i.e. before the ET to the BNC, contrary to the proposed model. In contrast, the study on the F → O transition, however, supports the transfer of the pumped proton to PLS upon ET to the binuclear center (Siletsky et al. 2004). These different results may suggest that the oxidative and reductive halves of the catalytic cycle are not entirely identical in all mechanistic details, besides the obvious difference in oxygen chemistry, the redox potential of metal centers and reaction kinetic rates. It should be noted that the scheme (Fig. 4) is entirely suitable for the oxidative phase of the catalytic cycle, and in a slightly modified form for the reductive part, as well (see Fig. S1 in *SM*). Namely, in the reductive part of the cycle, the steps 2 and 3 are coupled and occur simultaneously. Also step 5, the transfer of a proton to OH^- ligand in the BNC, is accompanied with the complete transfer of an electron to the Cu_B center.

The proton translocation from E242 to PLS upon the reduction of heme *a* is an endergonic step (Kaila et al. 2009; Quenneville et al. 2006), which could be facilitated by an initially generated small population of the reduced heme a_3 (Popovic and Stuchebrukhov 2012). The proton transfer to the PLS (during the O → E transition) considerably increases the redox potential of heme a_3, thereby stabilizing the electron at the BNC at the significant level, which in turn further increases the driving force for PT to the PLS. In other words, the increased population of the protonated His (PLS) gives rise to the reduced population of heme a_3, and vice versa. Therefore, one can say that the electron and the proton drive each other at this step to the more stable (intermediate) state of the enzyme where they

occupy heme a_3 (BNC) and H291 (PLS), respectively. This is a typical situation for a coupled electron and proton transfer reactions (Hammes-Schiffer and Stuchebrukhov 2010). Namely, without an electron, the proton transfer is unfavorable, likewise without the proton, electron transfer is unfavorable; however, transition of both electron and proton is favorable in energy. The transition in this case occurs in the course of thermal fluctuations and reflects the statistical and coupled nature of the reaction.

Proton and water exit

The proton and water exit pathways are the constitutive and important parts of the pumping mechanism in CcO. Little is experimentally known about the exit pathway and there may be multiple routes beyond the PLS toward the *P*-side (Hosler 2004; Mills and Ferguson-Miller 2002). Above the hemes on the interface between subunits I and II (see, Fig. 1a), a large number of scattered internal water molecules have been found in the crystal structures (Qin et al. 2006; Shinzawa-Itoh et al. 2007), making the identification of a single proton exit pathway even more difficult. The electrostatic calculations suggest that protons exit the enzyme by means of a discrete pathway and not by random diffusion (Popovic and Stuchebrukhov 2005). We proposed three putative proton exit paths with the following proton release groups—D51, $K171_{II}/D173_{II}$, and $H24_{II}/D25_{II}$. Non-conserved D51 was previously proposed as a proton release group in bovine CcO, based on the conformational changes of its side-chain in different redox states (Yoshikawa et al. 1998). However, the thermodynamic energy profiles favor the $K171_{II}/D173_{II}$ exit channel the most. The two other proton exit sites might be energetically competitive under some circumstances, although their involvement is much less likely than that of the strongly coupled $K171_{II}/D173_{II}$ pair (electrostatic coupling of 0.25 eV).

The main proton exit channel includes H291 (PLS), Wat1, PRA of heme a_3, D364, H368, and leads via internal water molecules and a redox-inactive Mg^{2+} center to $D173_{II}/K171_{II}$ exit point. Both highly conserved residues D364 and H368 are H-bonded to PRAa_3. In some studies, their role has shown to be crucial for proton translocation and catalytic activity (Das et al. 1999; Pfitzner et al. 1998), while in the other studies no significant effect has been found (Qian et al. 1997; Thomas et al. 1993). Alternatively, a proton might perhaps move along the oxygen atoms of the carboxylate and backbone carbonyl groups of PRAa_3, D364 and I365 to reach $K171_{II}$ site, 7.75Å away from the starting point (PRA:Oδ1–K171:Nζ). Movement of two adjacent water molecules closer to this area could facilitate such proton translocation.

In other aa_3-type of oxygen reductases, $K171_{II}$ and $D173_{II}$ residues are well-conserved and could have the same role. However, adjacent I365, located between D364 and $K171_{II}$ in bovine CcO, is replaced with R408 (*R. sphaeroides*) or R400 (*P. denitrificans*). Our model suggests that the main proton exit pathway in *R. sphaeroides* leads from the PLS to R408 and $D229_{II}/K227_{II}$ sites, while the equivalent R400 and $D193_{II}/K191_{II}$ sites could be the main proton release group in CcO from *P. denitrificans* (Popovic et al. 2010). Results from recent experimental studies indicate that protons may exit through a channel on the interface of subunits I and II leading from the catalytic site, via T294 and Mg-center to the *P*-side (Brzezinski, personal communication), in agreement with theoretical calculations (Popovic and Stuchebrukhov 2005). Namely, T294 (Thr377 in *R. sphaeroides* notation) is a part of the H-bonding network making multiple bonds with $D173_{II}$ residue, a H_2O molecule close to H368, and a weak H-bond with a H_2O ligand of Mg^{2+} center. Other study on the ba_3-type from *T. thermophilus* has shown that only D372I and H376N mutants (from all examined) retain relatively high turnover and normal spectral features, but do not pump protons (Chang et al. 2012). They assume that PRAa_3 or Wat1 are good candidates for the PLS, and their putative proton exit path is consistent with our proposal.

Water access from the outside of the enzyme and water escape from the buried active site were studied by an advanced time-resolved experimental technique (Schmidt et al. 2003). The results of this study suggest that water molecules formed in the catalytic site exit via Mg^{2+} center using most likely one distinct pathway. In theoretical study, the network of connected internal cavities is examined using structural analysis, MD simulations, and free energy calculations (Sugitani and Stuchebrukhov 2009). Two exit pathways, connecting the catalytic site via Mg^{2+} center to the *P*-side of the enzyme, have been identified. One pathway is leading via R438/R439 toward the Cu_A center, approaching closely its $H204_{II}$ ligand and $K171_{II}$ residue; and the other is leading toward D364 and T294. These pathways are well-conserved among different aa_3-type enzymes. It seems that the water exit pathways are closely related to the proton exit routes described above.

Free energy diagram

Energetics of proton and electron transfer reactions during the O → E transition is shown in Fig. 5 (Popovic, manuscript in preparation). The results are obtained from the combined DFT/electrostatic calculations and for the His291 pumping model shown schematically in Fig. 2. The obtained energy levels are fairly comparable with the results of the similar model, where PRAa_3 is considered as

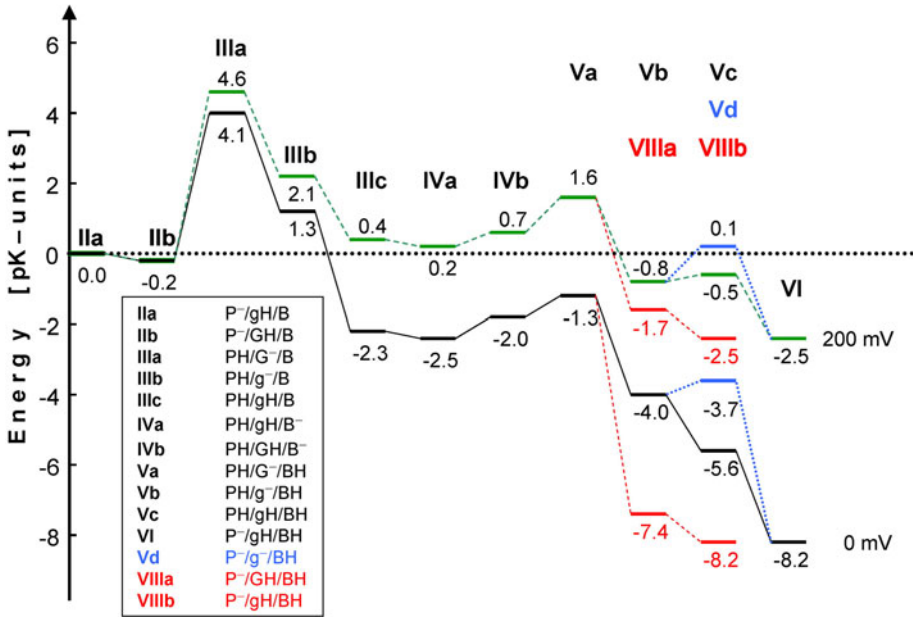

Fig. 5 Energy diagram of proton and electron transfer reaction steps during the O → E transition for the $\varepsilon_{prot}/\varepsilon_{cavity} = 4/20$ dielectric model. Thermodynamic levels are calculated without (*black*) and with (*green*) membrane potential gradient of 200 meV. Each state (II to VIII) is defined by the protonatation and redox state of H291/E242/BNC. PH and P^- are protonated and deprotonated form of H291 (PLS). gH, g^-, GH and G^- represent Glu in protonated and deprotonated state in *down* and *up* conformation. B, B^-, and BH are oxidized, reduced, and reduced-protonated forms of the binuclear center (BNC). The *red states* describe a possible proton leak (Va → VIIIa → VIIIb), where a proton flows back from PH to G^-, before G^- can flop down to g^- conformation and gets reprotonated through the D-channel. The leak is thermodynamically more favorable than the forward reaction but kinetic barrier for this back flow is too high (Kaila et al. 2009), due to repulsive interactions with the salt bridge and unfavorable orientation of internal water molecules in the hydrophobic cavity. Energetics of the proton pumping before or after the reprotonation of E242 is displayed by the steps Vb → Vd (*blue*) → VI or steps Vb → Vc → VI, respectively, energetically and kinetically favoring the latter situation

the PLS, see Fig. 6 in Kaila et al. (2009). Figure 4, in the same study, displays the kinetic energy barriers between the states of the enzyme during one proton pumping step. Transition state theory was employed for estimating activation energies (Δg^*) from the rate constant (k) of transitions, given as: $k = k_0 \exp(-\Delta g^*/k_B T)$. The state **Va** with the proton in the PLS (PRAa_3 or H291) is especially vulnerable to leak back to G^- site ($E242^-$ in upper conformation), instead of being released to the *P*-side of the membrane, which would result in a loss of proton pumping. This suggests that both kinetic and thermodynamic asymmetries in the position of the E242 side-chain play important roles in preventing such a leak. In addition, the transition states and kinetic barriers have been also explored in the recent computational studies (Blomberg and Siegbahn 2010; Olsson et al. 2007; Siegbahn and Blomberg 2007).

Obviously, there are more different control mechanisms and gating situations employed by the enzyme to ensure the unidirectionality of the proton translocation and to prevent proton leaks in the opposite direction. Several models have been proposed lately, discussing other aspects, alternative mechanisms, different gating situations and kinetic energy barriers, e.g. Blomberg and Siegbahn (2010); Brändén et al. (2006); Faxen et al. (2005); Kaila et al. (2008); Pisliakov et al. (2008); Popovic and Stuchebrukhov (2005); Sharpe and Ferguson-Miller (2008).

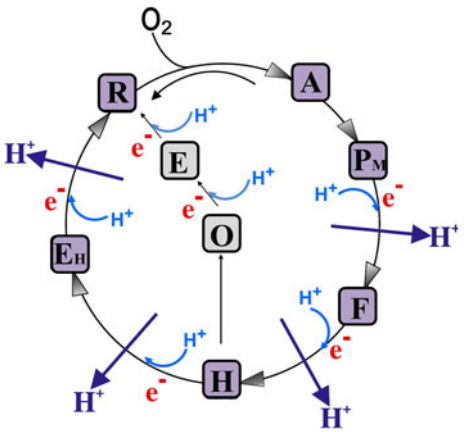

Fig. 6 The catalytic cycle of cytochrome *c* oxidase. The *squares* represent states of the heme a_3–Cu_B binuclear center. During regular turnover, one proton is pumped (*dark blue arrows*) from inside to outside of the membrane for each electron transferred (marked with e^-) to the BNC. Each electron transfer into the BNC is also linked to uptake of a *chemical* proton from the *N*-side (*light blue arrows*) and its translocation to the active site for the protonation of oxygen intermediates

H291 is also included as the PLS of the chemically explicit model (Sharpe and Ferguson-Miller 2008) for the pumping mechanism in CcO. Recent ATR-FTIR spectroscopic measurements suggest that His ligated to Cu_B center and exposed to the hydrophilic cavity, may go through a protonation change upon binding of formate to the BNC of bovine CcO (Iwaki and Rich 2004). These are rare experimental evidences that H291 might be involved in change of the protonation state, but the situation is not any better with the other potential proton-loading sites.

The presented model of proton pumping in CcO correlates well with most experimental data cited in this review paper. The "His291 pump model" is discussed and compared with the experimental results throughout the text. The model was initially developed based on results of the continuum electrostatics by calculating the electrostatic free energies from the solution of the LPBE, see e.g. (Couch et al. 2011; Popovic and Stuchebrukhov 2004a; Popovic et al. 2001, 2002). In-house developed QM/MM method, based on the combined DFT/electrostatic calculations (Makhov et al. 2006; Popovic et al. 2005; Quenneville et al. 2006), has been used to calculate more accurate energetics of the electron and proton transfer reactions. The applied methods also include the solvation energy calculations, molecular mechanics and MD simulations. Therefore, the model may reproduce well the thermodynamic properties of the enzyme, as for instance—pK_a values of titratable sites, the redox potential of the metal centers or the free energies of the proton and electron transfer reactions. However, from the thermodynamic energy profiles, one cannot judge about the activation energies of the transition states, kinetic barriers and reaction rate constants. Obtaining this important information for the "His291 pumping model" is currently underway and will be presented elsewhere.

The catalytic cycle

In the catalytic cycle, CcO undergoes through several states (R, A, P, F, H, O, E), which differ in the redox state of metal centers and the protonation state of the substrate and ligands in the binuclear complex. These different states can be detected by optical and spectroscopic methods, though in some particular cases, it is not possible to uniquely determine the protonation state of ligands and oxygen intermediates (Gennis 1998, 2004; Siletsky and Konstantinov 2012). In Fig. 6, the purple squares represent the states of the main cycle, whereas one can distinguish the oxidative (R → H) and reductive (H → R) halve. In the oxidative reaction phase, metal centers (Fe_{a3} and Cu_B) are oxidized providing three electrons for the total reduction of dioxygen, while the fourth electron is given by nearby Y244 covalently linked to H240 the ligand to Cu_B (Babcock 1999; Barry and Babcock 1987; Fabian et al. 1999; Hemp and Robinson 2006; Proshlyakov et al. 2000). In the reductive reaction phase, metal ions of the BNC get reduced by the incoming electrons supplied by cyt *c*. The oxidative phase begins at state R (reduced, Fe[II] Cu[I]), and continues with states A (oxygen adduct, Fe[II]–O_2 Cu[I]), P_M (peroxy, Fe[IV] = O Cu[II] Tyr-$O^{\cdot}$), F (ferryl, Fe[IV] = O Cu[II] tyr-O^{-}), and H (hydroxy, Fe[III] Cu[II]) (Proshlyakov et al. 2000). In the absence of an electron donor, the metastable oxidized H state may relax into state O (oxidized, Fe[III Cu[II]) (Antonini et al. 1977; Brunori et al. 1987), which may be reduced via state E (Fe[III] Cu[I]) back to state R (Bloch et al. 2004). However, during continuous turnover, the H state is reduced back to R via state E_H (Fe[III] Cu[I]). In the main cycle, both (oxidative and reductive) halves are coupled to pumping of two protons, one for each electron transfer into the BNC. Each electron transfer into the BNC is also linked to uptake of a substrate proton from the *N*-side and its translocation to the active site for the protonation of oxygen intermediates. However, after relaxation of H to O, there is no a proton pumping in the reductive phase (O → R). It is experimentally shown that the enzyme isolated in the oxidized state in anaerobic conditions, not recently undergone oxidation by O_2, does not pump protons (Belevich et al. 2006).

Efficiency of the proton pump

It should be noted that the cytochrome oxidase proton pump reactions are reversible (Siegbahn and Blomberg 2007; Wikström 1981) and therefore their activation energies and kinetic barriers are particularly important for the proper functioning of the enzyme. Proton pumping across the membrane is highly endergonic process and for that reason it needs to be coupled with the chemical reduction in the active site of the enzyme, which may provide enough energy. Based on the redox potential of the half-reactions, O_2/H_2O (E = 800 mV) and cytochrome *c* [Fe^{3+}/Fe^{2+}] (E = 300 mV), one can estimate the overall driving force of 500 meV per electron for the exergonic redox reaction. On the other hand, a translocation of the two electrical charges per electron, against the membrane potential of 200–220 mV, requires a work of 400–440 meV (Brzezinski and Gennis 2008). Accordingly, the efficiency of CcO as a proton pump is somewhere between 80–90 %, when it works with a full capacity, i.e. against the high values of the protonmotive force (*pmf*). The maximal turnover of CcO is then around 1000 e^{-}/s, i.e. 1000 H^{+} are pumped and 500 water molecules are produced every second. At high *pmf* there is an overall driving

force of only 60–100 meV per electron for the underlined coupled processes. Cytochrome oxidase operates relatively close to equilibrium between the driving and the driven reactions with high degree of efficiency and in that respect is a quite different from most other protein systems (e.g. bacteriorhodopsin or photosynthetic reaction center; Medvedev et al. 2008), where a substantial amount of energy is wasted as heat. However, operating close to equilibrium usually means a much higher risk of competing back reactions (leak of protons back into a pump). Also, it is shown that a work at high *pmf* is associated with the increased production of reactive oxygen species (ROS) such as superoxides and peroxides ($\cdot O_2^-$, H_2O_2, and $\cdot OH$), which may result in oxidative stress, serious damage of the mitochondrial membrane and cell death (Korshunov et al. 1997). Consequently, this puts high demands on the effectivity of kinetic gating mechanism. In other words, kinetic barriers need to be settled in such way to maintain the unidirectionality of the proton transport through the enzyme and to have a subtle control of the whole pumping process. Earlier study explored the mechanism of control of cytochrome oxidase activity by the electrochemical-potential gradient (Brunori et al. 1985).

Concluding remarks

Transmembrane electrochemical proton gradient is used to store free energy in biological systems, and subsequently to drive the synthesis of biomolecules, transmembrane transport and to provide energy for all other cell processes. These gradients are maintained by membrane-bound proton pumps that utilize free energy provided by electron transfer or light for proton transport through the enzyme. In recent years, their wild type and mutant structures have been solved indicating that both protein-bound internal water molecules and protonatable amino acid residues play central roles in transmembrane proton conduction. From these structures, in combination with functional and computational studies, have emerged general principles of proton transport across membranes and control mechanisms for such reactions, in particular with regard to the electron-transfer-driven proton pump cytochrome *c* oxidase.

The coupling of electron and proton transfer reactions plays a crucial role in CcO. During the course of the catalytic reduction of O_2, the redox changes of metal centers and protonation changes of protonatable ligands and oxygen intermediates take place in the binuclear Fe_{a3}/Cu_B center, the active site of the enzyme. They may further induce the alternation of H-bonds, reorientation of internal water molecules, the side-chain conformational and protonation changes of amino acid residues in the vicinity of the BNC, as for instance, in the hydrophobic cavity between the hemes or hydrophilic cavity above the Fe_{a3}/Cu_B center. Due to the long-range electrostatic interactions, the influence could be extended to the entrance K- and D-channel or proton/water exit channel(s). It is shown that site-directed mutations in the D-channel, far away from the active site, BNC or PLS, may for instance impair a proton pumping while still retaining the enzyme turnover. This suggests that in cytochrome oxidase there is a subtle kinetic control of the coupled electron and proton transfer reactions, which also involves internal protein-bound water molecules.

Acknowledgments I would like to thank Prof. Ivan Juranić for helpful discussion and careful reading of the manuscript. This work is supported by Ministry of Education, Science and Technological Development of Serbia, research grant 172035. The author is grateful to Prof. Alexei Stuchebrukhov for successful collaboration over the years on the cytochrome oxidase project. I am also grateful to the referee for pointing my attention to several references and on the related comments.

Conflict of interest The author declares that he has no conflict of interest.

References

Abramson J, Riistama S, Larsson G, Jasaitis A, Svensson-Ek M et al (2000) The structure of the ubiquinol oxidase from Escherichia coli and its ubiquinone binding site. Nature Struct Biol 7:910–917

Ädelroth P, Svensson-Ek M, Mitchell DM, Gennis RB, Brzezinski P (1997) Glutamate 286 in cytochrome aa3 from Rhodobacter sphaeroides is involved in proton uptake during the reaction of the fully-reduced enzyme with dioxygen. Biochemistry 36:13824–13829

Ädelroth P, Gennis RB, Brzezinski P (1998) Role of the pathway through K(I-362) in proton transfer in cytochrome c oxidase from R. sphaeroides. Biochemistry 37:2470–2476

Agmon M (1995) The Grotthuss mechanism. Chem Phys Lett 244: 456–462

Ali-Torres J, Rodriguez-Santiago L, Sodupe M (2011) Computational calculations of pK(a) values of imidazole in Cu(II) complexes of biological relevance. Phys Chem Chem Phys 13:7852–7861

Antonini E, Brunori M, Greenwood C, Malmström BG (1970) Catalytic mechanism of cytochrome oxidase. Nature 228: 936–937

Antonini E, Brunori M, Colosimo A, Greenwood C, Wilson MT (1977) Oxygen 'pulsed' cytochrome c oxidase: functional properties and catalytic relevance. Proc Natl Acad Sci USA 74:3128–3132

Babcock GT (1999) How oxygen is activated and reduced in respiration. Proc Natl Acad Sci USA 96:12971–12973

Babcock GT, Wikström M (1992) Oxygen activation and the conservation of energy in cell respiration. Nature 356:301–309

Barry BA, Babcock GT (1987) Tyrosine radicals are involved in the photosynthetic oxygen-evolving systems. Proc Natl Acad Sci USA 84:7099–7103

Belevich I, Verkhovsky MI, Wikström M (2006) Proton-coupled electron transfer drives the proton pump of cytochrome c oxidase. Nature 440:829–832

Belevich I, Bloch DA, Belevich N, Wikström M, Verkhovsky MI (2007) Exploring the proton pump mechanism of cytochrome c oxidase in real time. Proc Natl Acad Sci USA 104:2685–2690

Bloch D, Belevich I, Jasaitis A, Ribacka C, Puustinen A et al (2004) The catalytic cycle of cytochrome c oxidase is not the sum of its two halves. Proc Natl Acad Sci USA 101:529–533

Blomberg MR, Siegbahn PEM (2010) A quantum chemical study of the mechanism for proton-coupled electron transfer leading to proton pumping in cytochrome c oxidase. Mol Phys 108:2733–2743

Brändén M, Sigurdson H, Namslauer A, Gennis RB, Ädelroth P, Brzezinski P (2001) On the role of the K-proton transfer pathway in cytochrome coxidase. Proc Natl Acad Sci USA 98:5013–5018

Brändén M, Tomson F, Gennis RB, Brzezinski P (2002) The entry point of the K-proton transfer pathway in cytochrome c oxidase. Biochemistry 41:10794–10798

Brändén G, Brändén M, Schmidt B, Mills DA, Ferguson-Miller S, Brzezinski P (2005) The protonation state of a heme propionate controls electron transfer in cytochrome c oxidase. Biochemistry 44:10466–10474

Brändén G, Pawate AS, Gennis RB, Brzezinski P (2006) Controlled uncoupling and recoupling of proton pumping in cytochrome c oxidase. Proc Natl Acad Sci USA 103:317–322

Brunori M, Sarti P, Colosimo A, Antonini G, Malatesta F et al (1985) Mechanism of control of cytochrome oxidase activity by the electrochemical-potential gradient. EMBO J 4:2365–2368

Brunori M, Antonini G, Malatesta F, Sarti P, Wilson MT (1987) Cytochrome-c oxidase. Eur J Biochem 169:1–8

Brzezinski P (2004) Redox-driven membrane-bound proton pumps. Trends Biochem Sci 29:380–387

Brzezinski P, Ädelroth P (2006) Design principles of proton-pumping haem-copper oxidases. Curr Opin Struct Biol 16:465–472

Brzezinski P, Gennis RB (2008) Cytochrome c oxidase: exciting progress and remaining mysteries. J Bioenerg Biomembr 40:521–531

Chakrabarty S, Warshel A (2013) Capturing the energetics of water insertion in biological systems: the water flooding approach. Proteins 81:93–106

Chakrabarty S, Namslauer I, Brzezinski P, Warshel A (2011) Exploration of the cytochrome c oxidase pathway puzzle and examination of the origin of elusive mutational effects. Biochim Biophys Acta 1807:413–426

Chang HY, Choi SK, Vakkasoglu AS, Chen Y, Hemp J et al (2012) Exploring the proton pump and exit pathway for pumped protons in cytochrome ba(3) from Thermus thermophilus. Proc Natl Acad Sci USA 109:5259–5264

Couch V, Popovic D, Stuchebrukhov A (2011) Redox-coupled protonation of respiratory complex I: the hydrophilic domain. Biophys J 101:431–438

Das TK, Gomes CM, Teixeira M, Rousseau DL (1999) Redox-linked transient deprotonation at the binucear site in the aa3-type quinol oxidase from Acidianus ambivalens: implications for proton translocation. Proc Natl Acad Sci USA 96:9591–9596

Dürr KL, Koepke J, Hellwig P, Müller H, Angerer H et al (2008) A D-pathway mutation decouples the Paracoccus denitrificans cytochrome c oxidase by altering the side-chain orientation of a distant conserved glutamate. J Mol Biol 384:865–877

Fabian M, Wong WW, Gennis RB, Palmer G (1999) Mass spectrometric determination of dioxygen bond splitting in the ''peroxy'' intermediate of cytochrome c oxidase. Proc Natl Acad Sci USA 96:13114–13117

Fadda E, Yu C-H, Pomès R (2008) Electrostatic control of proton pumping in cytochrome c oxidase. Biochim Biophys Acta 1777:277–284

Faxen K, Gilderson G, Ädelroth P, Brzezinski P (2005) A mechanistic principle for proton pumping by cytochrome c oxidase. Nature 437:286–289

Ferguson-Miller S, Babcock GT (1996) Heme-copper oxidase. Chem Rev 7:2889–2907

Fetter JR, Sharpe M, Qian J, Mills D, Ferguson-Miller S, Nicholls P (1996) Fatty acids stimulate activity and restore respiratory control in a proton channel mutant of cytochrome c oxidase. FEBS Lett 393:155–160

Gennis RB (1998) How does cytochrome oxidse pump protons? Proc Natl Acad Sci USA 95:12747–12749

Gennis RB (2004) Coupled proton and electron transfer reactions in cytochrome oxidase. Front Biosci 9:581–591

Ghosh N, Prat-Resina X, Gunner MR, Cui Q (2009) Microscopic pK(a) analysis of Glu286 in cytochrome c oxidase (Rhodobacter sphaeroides): toward a calibrated molecular model. Biochemistry 48:2468–2485

Hammes-Schiffer S, Stuchebrukhov AA (2010) Theory of coupled electron and proton transfer reactions. Chem Rev 110:6939–6960

Han S, Takahashi S, Rousseau DL (2000) Time dependence of the catalytic intermediates in cytochrome c oxidase. J Biol Chem 275:1910–1919

Han D, Namslauer A, Pawate A, Morgan JE, Nagy S et al (2006) Replacing Asn207 by aspartate at the neck of the D channel in the aa(3)-type cytochrome c oxidase from Rhodobacter sphaeroides results in decoupling the proton pump. Biochemistry 45:14064–14074

Hellwig P, Behr J, Ostermeier C, Richter OM, Pfitzner U et al (1998) Involvement of glutamic acid 278 in the redox reaction of the cytochrome c oxidase from Paracoccus denitrificans investigated by FT-IR spectroscopy. Biochemistry 37:7390–7399

Hemp J, Robinson DE (2006) Evolutionary migration of a posttranslationally modified active-site residue in the proton-pumping heme–copper oxygen reductases. Biochemistry 45:15405–15410

Henry RM, Caplan D, Fadda E, Pomès R (2011) Molecular basis of proton uptake in single and double mutants of cytochrome c oxidase. J Phys Condens Matter 23:4102–4110

Hosler JP (2004) The influence of subunit III of cytochrome c oxidase on the D pathway, the proton exit pathway and mechanism-based inactivation in subunit I. Biochim Biophys Acta 1655:332–339

Hosler JP, Shapleigh JP, Mitchell DM, Kim Y, Pressler MA et al (1996) Polar residues in helix VIII of subunit I of cytochrome c oxidase influence the activity and the structure of the active site. Biochemistry 35:10776–10783

Hosler JP, Ferguson-Miller S, Mills DA (2006) Energy transduction: proton transfer through the respiratory complexes. Annu Rev Biochem 75:165–187

Iwaki M, Rich PR (2004) Direct detection of formate ligation in cytochrome c oxidase by ATR-FTIR spectroscopy. J Am Chem Soc 126:2386–2389

Iwata S, Ostermeier C, Ludwig B, Michel H (1995) Structure at 2.8 Å resolution of cytochrome c oxidase from Paracoccus denitrificans. Nature 376:660–669

Jasaitis A, Verkhovsky MI, Morgan JE, Verkhovskaya ML, Wikström M (1999) Assignment and charge translocation stoichiometries of the electrogenic phases in the reaction of cytochrome c with dioxygen. Biochemistry 38:2697–2706

Johansson AL, Chakrabarty S, Berthold CL, Högbom M, Warshel A, Brzezinski P (2011) Proton-transport mechanisms in cytochrome c oxidase revealed by studies of kinetic isotope effects. Biochim Biophys Acta 1807:1083–1094

Johansson AL, Carlsson J, Högbom M, Hosler JP, Gennis RB, Brzezinski P (2013) Proton uptake and pKa changes in the uncoupled Asn139Cys variant of cytochrome c oxidase. Biochemistry 52:827–836

Kaila VRI, Verkhovsky MI, Hummer G, Wikström M (2008) Glutamic acid 242 is a valve in the proton pump of cytochrome c oxidase. Proc Natl Acad Sci USA 105:6255–6259

Kaila VRI, Verkhovsky MI, Hummer G, Wikström M (2009) Mechanism and energetics by which glutamic acid 242 prevents leaks in cytochrome c oxidase. Biochim Biophys Acta 1787: 1205–1214

Karpefors M, Ädelroth P, Aagaard A, Smirnova IA, Brzezinski P (1999) The deuterium isotope effect as a tool to investigate enzyme catalysis: proton-transfer control mechanisms in cytochrome c oxidase. Isr J Chem 39:427–437

Kirchberg K, Michel H, Alexiev U (2013) Exploring the entrance of proton pathways in cytochrome c oxidase from Paracoccus denitrificans: surface charge, buffer capacity and redox-dependent polarity changes at the internal surface. Biochim Biophys Acta 1827:276–284

Konstantinov AA, Siletsky S, Mitchell D, Kaulen A, Gennis RB (1997) The role of the two proton input channels in cytochrome c oxidase from Rhodobacter Sphaeroides probed by the effects of site-directed mutations on time-resolved electrogenic intraprotein proton transfer. Proc Natl Acad Sci USA 94:9085–9090

Korshunov SS, Skulachev VP, Starkov AA (1997) High protonic potential actuates a mechanism of production of reactive oxygen species in mitochondria. FEBS Lett 416:15–18

Lee HM, Das DL, Rousseau DA, Mills S, Ferguson-Miller RB (2000) Mutations in the putative H-channel in the cytochrome c oxidase from Rhodobacter sphaeroides show that this channel is not important for proton conduction but reveal modulation of the properties of heme a. Biochemistry 39:2989–2996

Lee HJ, Ojemyr L, Vakkasoglu A, Brzezinski P, Gennis RB (2009) Properties of Arg481 mutants of the aa(3)-type cytochrome c oxidase from Rhodobacter sphaeroides suggest that neither R481 nor the nearby D-propionate of heme a(3) is likely to be the proton loading site of the proton pump. Biochemistry 48: 7123–7131

Luna VM, Chen Y, Fee JA, Stout CD (2008) Crystallographic studies of Xe and Kr binding within the large internal cavity of cytochrome ba3 from Thermus thermophilus: structural analysis and role of oxygen transport channels in the heme–Cu oxidases. Biochemistry 47:4657–4665

Makhov DV, Popovic DM, Stuchebrukhov AA (2006) Improved density functional theory/electrostatic calculation of the His291 protonation state in cytochrome c oxidase: self-consistent charges for solvation energy calculation. J Phys Chem B 110: 12162–12166

Medvedev ES, Kotelnikov A, Barinov AV, Psikha BL, Ortega JM et al (2008) Protein dynamics control of electron transfer in photosynthetic reaction centers from Rps. sulfoviridis. J Phys Chem B 112:3208–3216

Michel H (1998) The mechanism of proton pumping by cytochrome c oxidase. Proc Natl Acad Sci USA 95:12819–12824

Mills DA, Ferguson-Miller S (2002) Influence of structure, pH and membrane potential on proton movement in cytochrome oxidase. Biochim Biophys Acta 1555:96–100

Mills DA, Florens L, Hiser C, Qian J, Ferguson-Miller S (2000) Where is "outside" in cytochrome c oxidase and how and when do protons get there? Biochim Biophys Acta 1458:180–187

Mills DA, Tan Z, Ferguson-Miller S, Hosler J (2003) A role for subunit III in proton uptake into the D pathway and a possible proton exit pathway in Rhodobacter sphaeroides cytochrome c oxidase. Biochemistry 42:7410–7417

Noor MR, Soulimane T (2013) Structure of caa 3 cytochrome c oxidase – a nature-made enzyme-substrate complex. Biol Chem 394:579–591

Olkhova E, Hutter MC, Lill MA, Helms V, Michel H (2004) Dynamic water networks in cytochrome c oxidase from Paracoccus denitrificans investigated by molecular dynamics simulations. Biophys J 86:1873–1889

Olsson MHM, Warshel A (2006) Monte Carlo simulations of proton pumps: on the working principles of the biological valve that controls proton pumping in cytochrome c oxidase. Proc Natl Acad Sci USA 103:6500–6505

Olsson MHM, Siegbahn PEM, Blomberg MRA, Warshel A (2007) Exploring pathways and barriers for coupled ET/PT in cytochrome c oxidase: a general framework for examining energetics and mechanistic alternatives. Biochim Biophys Acta 1767: 244–260

Ostermeier C, Harrenga A, Ermler U, Michel H (1997) Structure at 2.7 Å resolution of the Paracoccus denitrificans two-subunit cytochrome c oxidase complexed with an antibody Fv fragment. Proc Natl Acad Sci USA 94:10547–10553

Pawate AS, Morgan J, Namslauer A, Mills D, Brzezinski P et al (2002) A mutation in subunit I of cytochrome oxidase from Rhodobacter sphaeroides results in an increase in steady-state activity but completely eliminates proton pumping. Biochemistry 41:13417–13423

Pereira MM, Santana M, Teixeira M (2001) A novel scenario for the evaluation of haem-copper oxygen reductases. Biochim Biophys Acta 1505:185–208

Pereira MM, Sousa FL, Veríssimo AF, Teixeira M (2008) Looking for the minimum common denominator in haem-copper oxygen reductases: towards a unified catalytic mechanism. Biochim Biophys Acta 1777:929–934

Pfitzner U, Odenwald A, Ostermann T, Weingard L, Ludwig B, Richter O-MH (1998) J Bioenerg Biomembr 30:89–97

Pfitzner U, Hoffmeier K, Harrenga A, Kannt A, Michel H et al (2000) Tracing the D-pathway in reconstituted site-directed mutants of cytochrome c oxidase from Paracoccus denitrificans. Biochemistry 39:6756–6762

Pisliakov AV, Sharma PK, Chu ZT, Haranczyk M, Warshel A (2008) Electrostatic basis for the unidirectionality of the primary proton transfer in cytochrome c oxidase. Proc Natl Acad Sci USA 105:7726–7731

Popovic DM, Stuchebrukhov AA (2004a) Electrostatic study of proton pumping mechanism of bovine heart cytochrome c oxidase. J Am Chem Soc 126:1858–1871

Popovic DM, Stuchebrukhov AA (2004b) Proton pumping mechanism and catalytic cycle of cytochrome c oxidase: coulomb pump model with kinetic gating. FEBS Lett 566:126–130

Popovic DM, Stuchebrukhov AA (2005) Proton exit channels in bovine cytochrome c oxidase. J Phys Chem B 109:1999–2006

Popovic DM, Stuchebrukhov AA (2006) Two conformational states of Glu242 and pKas in bovine cytochrome c oxidase. Photochem Photobiol Sci 5:611–620

Popovic DM, Stuchebrukhov AA (2012) Coupled electron and proton transfer reactions during the O → E transition in bovine cytochrome c oxidase. Biochim Biophys Acta 1817:506–517

Popovic DM, Zaric SD, Rabenstein B, Knapp EW (2001) Artificial cytochrome b: computer modeling and evaluation of redox potentials. J Am Chem Soc 123:6040–6053

Popovic DM, Zmiric A, Zaric SD, Knapp EW (2002) Energetics of radical transfer in DNA photolyase. J Am Chem Soc 124: 3775–3782

Popovic DM, Quenneville J, Stuchebrukhov AA (2005) DFT/electrostatic calculations of pKa values in cytochrome c oxidase. J Phys Chem B 109:3616–3626

Popovic DM, Leontyev IV, Beech DG, Stuchebrukhov AA (2010) Similarity of cytochrome c oxidases in different organisms. Proteins Struct Funct Bioinform 78:2691–2698

Proshlyakov DA, Pressler MA, DeMaso C, Leykam JF, DeWitt DL, Babcock GT (2000) Oxygen activation and reduction in respiration: involvement of redox-active tyrosine 244. Science 290:1588–1591

Qian J, Shi W, Pressler M, Hogansson C, Mills D et al (1997) Aspartate-407 in Rhodobacter sphaeroides cytochrome c oxidase is not required for proton pumping or manganese binding. Biochemistry 36:2539–2543

Qin L, Hiser C, Mulichak A, Garavito RM, Ferguson-Miller S (2006) Identification of conserved lipid/detergent binding sites in a high-resolution structure of the membrane protein cytochrome c oxidase. Proc Natl Acad Sci USA 103:16117–16122

Qin L, Liu J, Mills DA, Proshlyakov DA, Hiser C, Ferguson-Miller S (2009) Redox-dependent conformational changes in cytochrome c oxidase suggest a gating mechanism for proton uptake. Biochemistry 48:5121–5130

Quenneville J, Popovic DM, Stuchebrukhov AA (2004) Redox-dependent pKa of CuB histidine ligand in cytochrome c oxidase. J Phys Chem B 108:18383–18389

Quenneville J, Popovic DM, Stuchebrukhov AA (2006) Combined DFT and electrostatics study of the proton pumping mechanism in cytochrome c oxidase. Biochim Biophys Acta 1757: 1035–1046

Rich PR (1995) Towards an understanding of the chemistry of oxygen reduction and proton translocation in the iron-copper respiratory oxidases. Aust J Plant Physiol 22:479–486

Riistama S, Hummer G, Puustinen A, Dyer BR, Woodruff WH, Wikström M (1997) Bound water in proton translocation mechanism of the heme-copper oxidase. FEBS Lett 414: 275–280

Ruitenberg M, Kannt A, Bamberg E, Ludwig B, Michel H, Fendler K (2000) Single-electron reduction of the oxidized state is coupled to proton uptake via the K pathway in Paracoccus denitrificans cytochrome c oxidase. Proc Natl Acad Sci USA 97:4632–4636

Ruitenberg M, Kannt A, Bamberg E, Fendler K, Michel H (2002) Reduction of cytochrome c oxidase by a second electron leads to proton translocation. Nature 417:99–102

Salje J, Ludwig B, Richter OM (2005) Is a third proton-conducting pathway operative in bacterial cytochrome c oxidase? Biochem Soc Trans 33:829–831

Salomonsson L, Faxen K, Ädelroth P, Brzezinski P (2005) The timing of proton migration in membrane-reconstituted cytochrome c oxidase. Proc Natl Acad Sci USA 102:17624–17629

Salomonsson L, Brändén G, Brzezinski P (2008) Deuterium isotope effect of proton pumping in cytochrome c oxidase. Biochim Biophys Acta 1777:343–350

Sarti P, Forte E, Mastronicola D, Giuffrè A, Arese M (2012) Cytochrome c oxidase and nitric oxide in action: molecular mechanisms and pathophysiological implications. Biochim Biophys Acta 1817:610–619

Schmidt B, McCracken J, Ferguson-Miller S (2003) A discrete water exit pathway in the membrane protein cytochrome c oxidase. Proc Natl Acad Sci USA 100:15539–15542

Sharpe MA, Ferguson-Miller S (2008) A chemically explicit model for the mechanism of proton pumping in heme–copper oxidases. J Bioenerg Biomembr 40:541–549

Shimokata K, Katayama Y, Murayama H, Suematsu M, Tsukihara T et al (2007) The proton pumping pathway of bovine heart cytochrome c oxidase. Proc Natl Acad Sci USA 104:4200–4205

Shinzawa-Itoh K, Aoyama H, Muramoto K, Terada H, Kurauchi T et al (2007) Structures and physiological roles of 13 integral lipids of bovine heart cytochrome c oxidase. EMBO J 26:1713–1725

Siegbahn PEM, Blomberg MR (2007) Energy diagrams and mechanism for proton pumping in cytochrome c oxidase. Biochim Biophys Acta 1767:1143–1156

Siletsky SA, Konstantinov AA (2012) Cytochrome c oxidase: charge translocation coupled to single-electron partial steps of the catalytic cycle. Biochim Biophys Acta 1817:476–488

Siletsky SA, Pawate AS, Weiss K, Gennis RB, Konstantinov AA (2004) Transmembrane charge separation during the ferryl-oxo to oxidized transition in a nonpumping mutant of cytochrome c oxidase. J Biol Chem 279:52558–52565

Soulimane T, Buse G, Bourenkov GP, Bartunik HD, Huber R, Than ME (2000) Structure and mechanism of the aberrant ba(3)-cytochrome c oxidase from thermus thermophilus. EMBO J 19:1766–1776

Stuchebrukhov AA (2003) Electron transfer reactions coupled to proton translocation. Cytochrome oxidase, proton pumps, and biological energy transduction. J Theor Comp Chem 2:91–118

Stuchebrukhov AA, Popovic DM (2006) Comment on "acidity of a Cu-bound histidine in the binuclear center of cytochrome c oxidase". J Phys Chem B 110:17286–17287

Sugitani R, Stuchebrukhov AA (2009) Molecular dynamics simulation of water in cytochrome c oxidase reveals two water exit pathways and the mechanism of transport. Biochim Biophys Acta 1787:1140–1150

Sugitani R, Medvedev ES, Stuchebrukhov AA (2008) Theoretical and computational analysis of the membrane potential generated by cytochrome c oxidase upon single electron injection into the enzyme. Biochim Biophys Acta 1777:1129–1139

Svensson-Ek M, Abramson J, Larsson G, Tornroth S, Brzezinski P, Iwata S (2002) The x-ray crystal structures of wild-type and EQ(I-286) mutant cytochrome c oxidases from Rhodobacter Sphaeroides. J Mol Biol 321:329–335

Tashiro M, Stuchebrukhov AA (2005) Thermodynamic properties of internal water molecules in the hydrophobic cavity around the catalytic center of cytochrome c oxidase. J Phys Chem B 109:1015–1022

Thomas JW, Puustinen A, Alben JO, Gennis RB, Wikström M (1993) Substitution of asparagine for aspartate-135 in subunit I of the cytochrome bo ubiquinol oxidase of Escherichia Coli eliminates proton pumping activity. Biochemistry 32:10923–10928

Tsukihara T, Aoyama H, Yamashita E, Tomizaki T, Yamaguchi H et al (1996) The whole structure of the 13-subunit oxidized cytochrome c oxidase at 2.8 Å. Science 272:1136–1144

Tsukihara T, Shimokata K, Katayama Y, Shimada H, Muramoto K et al (2003) The low-spin heme of cytochrome c oxidase as the driving element of the proton-pumping process. Proc Natl Acad Sci USA 100:15304–15309

Vakkasoglu AS, Morgan JE, Han D, Pawate AS, Gennis RB (2006) Mutations which decouple the proton pump of the cytochrome c oxidase from Rhodobacter sphaeroides perturb the environment of glutamate 286. FEBS Lett 580:4613–4617

Vygodina TV, Pecoraro C, Mitchell D, Gennis R, Konstantinov AA (1998) Mechanism of inhibition of electron transfer by amino acid replacement K362 M in a proton channel of Rhodobacter sphaeroides cytochrome c oxidase. Biochemistry 37:3053–3061

Wikström M (1977) Proton pump coupled to cytochrome c oxidase in mitochondria. Nature 266:271–273

Wikström M (1981) Energy-dependent reversal of the cytochrome oxidase reaction. Proc Natl Acad Sci USA 78:4051–4054

Wikström M (2000) Mechanism of proton translocation by cytochrome c oxidase: a new four-stroke histidine cycle. Biochim Biophys Acta 1458:188–198

Wikström M (2004) Cytochrome c oxidase: 25 years of the elusive proton pump. Biochim Biophys Acta 1655:241–247

Wikström M, Verkhovsky MI (2007) Mechanism and energetics of proton translocation by the respiratory heme–copper oxidases. Biochim Biophys Acta 1767:1200–1214

Wikström M, Jasaitis A, Backgren C, Puustinen A, Verkhovsky MI (2000) The role of the D- and K-pathways of proton transfer in the function of the heam-copper oxidases. Biochim Biophys Acta 1459:514–520

Wikström M, Verkhovsky MI, Hummer G (2003) Water-gated mechanism of proton translocation by cytochrome c oxidase. Biochim Biophys Acta 1604:61–65

Wikström M, Ribacka C, Molin M, Laakkonen L, Verkhovsky M, Puustinen A (2005) Gating of proton and water transfer in the respiratory enzyme cytochrome c oxidase. Proc Natl Acad Sci USA 102:10478–10481

Xu JC, Voth GA (2006) Free energy profiles for H + conduction in the D-pathway of cytochrome c oxidase: a study of the wild type and N98D mutant enzymes. Biochim Biophys Acta 1757: 852–859

Yang S, Cui Q (2011) Glu-286 rotation and water wire reorientation are unlikely the gating elements for proton pumping in cytochrome c oxidase. Biophys J 101:61–69

Yoshikawa S, Shinzawa-Itoh K, Nakashima R, Yaono R, Yamashita E et al (1998) Redox-coupled structural changes in bovine heart cytochrome c oxidase. Science 280:1723–1729

Zaslavsky D, Gennis RB (2000) Proton pumping by cytochrome oxidase: progress, problems and postulates. Biochim Biophys Acta 1458:164–179

Zaslavsky D, Kaulen AD, Smirnova IA, Vygodina T, Konstantinov AA (1993) Flash-induced membrane potential generation by cytochrome c oxidase. FEBS Lett 336:389–393

Zheng X, Medvedev DM, Swanson J, Stuchebrukhov AA (2003) Computer simulation of water in cytochrome c oxidase. Biochim Biophys Acta 1557:99–107